fMRI PROCESSING TOOL FOR THE ANALYSIS, PARAMETRISATION AND COMPARISON OF PREPROCESSED SPM IMAGES

Álvaro Muro, Begoña García Zapirain, Amaia Méndez, Ibon Ruiz

University of Deusto
Avda/Universidades 24, 48007 Bilbao, Spain
alvaro.muro@deusto.es, { mbgarcia, amendez, ibruiz}@eside.deusto.es

ABSTRACT

The main purpose of this work is to develop an analysis tool to evaluate differences in brain activation during specific tasks in neurologically disabled patients versus a non-impaired control group. The database will include a set of fRMI images obtained by a Siemens Avanto 1.5 T machine. The main idea of the authors has been to develop a system combining processed fRMI images from SPM software with an image processing algorithm to obtain neuronal activation regions, measure perimeters and areas and perform comparisons between tests, in order to quantitatively evaluate the initial situation of the patient as well as to monitor his/her evolution. Future work will extend the use of the application for a wider range of neurological disorders, and integrate EEG studies as a complementary tool for diagnosis.

Index Terms— Image Processing, fMRI, SPM

1. INTRODUCTION

The neuropsychological disorders most frequent in children are dyslexia and Attention Deficit & Hyperactivity Disorder (ADHD), pathologies which are usually chronic and persistent. According to studies carried out in the USA and EU, the percentage of child dyslexia occurrence is 5-17% [1] and 3 to 5% for ADHD with symptoms starting before seven years of age [2]. We now have several non-invasive neuro-imaging diagnose techniques such as Positron Emission Tomography (PET)[3], magneto encephalography (MEG)[4] and Functional Magnetic Resonance (fMRI) [5] [6], which have contributed to understanding these pathologies in the functional and morphological fields. These techniques differ on a spatial and temporal resolution degree, fMRI being the one with the best spatial resolution.

fMRI has had a profound impact on neuroscience since the initial activation of the visual cortex by Belliveau in 1991. fMRI signal production is due to the paramagnetic effect of oxyhemoglobin. The brain's focal activation results in an increase in flow, oxygen distribution and brain volume. The relation between oxyhemoglobin and deoxyhemoglobin in venous blood increases and, as a result, the blood and tissues have less susceptibility, which causes a higher signal measurable on T2 and T2* images. This is known as blood oxygen level-dependent (BOLD).

The main aim of this work is to aid specialists in their daily practice by providing them with a tool to objectively evaluate neurological diseases using fMRI signal-processing algorithms. This being the main aim, a number of secondary objectives could also be achieved:

- To create a complete database with records of fMRI images.
- To develop an image processing algorithm for the adequate segmentation of images for the calculation of external and internal contours of the area of interest.
- To calculate the numerical value of objective parameters that enable analysis of differences in brain activation during reading tasks in neurologically disabled children as opposed to non-impaired controls. A report will be prepared including quantitative parameters, images, external and internal contours and clinical parameters. In addition, a figure will clearly represent all the parameters, as well as the normal regions and those of interest.

This paper is divided into the following principal sections: Section 2 describes the used methodology, section 3 presents the proposed system, section 4 describes the results obtained, and section 5 presents the authors' conclusions and future work.

2. DATABASE

In order to develop and test the implemented algorithms, a database containing functional and structural magnetic resonance images was created. The acquisition device was a Siemens Magnetom Avanto 1.5 Tesla property of Osatek Ltd. at Galdakao Hospital, controlled by radiologists Alberto Cabrera and Ibone Saralegui. Two different types of images were acquired for each subject: anatomical or structural images and functional images. The scanner configuration parameters for structural images were TR =1900ms (Repetition Time), TE =2.95ms (Echo Time) and SL =1mm (Slice Thickness). Image resolution was 256x256x176 pixels with a voxel size of 1x0.977x0.977. For functional images the parameter values were TR=3000ms, TE=50ms, and SL=3mm. Image resolution was 64x64x29 pixels with voxel size 3x3x4.05. All the data collected from the scanner was coded in Siemens Magnetom proprietary format.

12 subjects between 9 and 11 years old were scanned for the purpose of the study. Two of them were male subjects and ten female. The control group is formed by eleven of these subjects. The twelfth subject was not included, being classified as a case with undiagnosed but probable dyslexia. The

 ISSN 2076-1465

12 subjects performed 5 different task paradigms involving the use of language understanding and generation areas (Broca and Wernicke, or Brodmann's 44-45 and 22 respectively), where differences between control and patient groups are expected. A total of 75 tests were carried out, 12 of which had 110 complete brain volume scans and the remaining 63 had 90 volumes each, making a total of 6990 volumes scanned for the database.

3. TECHNICAL METHODS

The main objective of this study is to extract the relevant information from the fMRI slices and to take a number of measurements, in order to check similarities and differences between the neural activation areas belonging to control group subjects and those belonging to dyslexic patients. We have used the following techniques to process the data, which can be grouped into two sets: SPM8 fMRI analysis techniques [7] and image processing methods.

2.1 Rigid Body registration

This technique is used in order to reduce the effect of subject movement during the acquisition of the scans and to model different head positions of the same subject. It uses generalized interpolation, where the images are first transformed before applying the local convolution. Generalized interpolation methods model an image as a linear combination of basis functions with local support, typically B-splines or o-Moms (maximal-order interpolation of minimal support) basis functions.

$$\beta^n(x) = \sum_{j=0}^{n} \frac{(-1)^j (n+1)}{(n+1-j)!\,j!} \max\left(\frac{n+1}{2} + x - j, 0\right)^n \quad (1)$$

Rigid-body transformations consist of only rotations and translations, and leave given arrangements unchanged. They are a subset of the more general affine transformations. For each point (x1; x2; x3) in an image, an affine mapping can be defined into the co-ordinates of another space (y1; y2; y3), applying a simple matrix multiplication (y=Mx).

2.2 Spatial Normalization using basis functions

When a study involves group analysis or inter-subject comparison, it is necessary to register the images of different subjects into roughly the same co-ordinate system, where the co-ordinate system is defined by a template image (or series of images). The method only uses up to a few hundred parameters, so can only model global brain shape. It works by estimating the optimum coefficients for a set of bases, by minimizing the sum of squared differences between the template and source image, while simultaneously maximizing the smoothness of the transformation using a maximum a posteriori (MAP) approach.

$$q^{(n+1)} = \left({C_0}^{-1} + A^T A/_{\sigma^2}\right)^{-1} \left({C_0}^{-1} q_0 + A^T A q^{(n)}/_{\sigma^2} - A^T b/_{\sigma^2}\right) \quad (2)$$

The algorithm starts with a 12 DF affine registration, followed by 3 translations, 3 rotations, 3 zooms and 3 shears. Afterwards, it fits overall shape and size and refines the registration with non-linear deformations. The algorithm simultaneously minimizes mean-squared difference (Gaussian likelihood) and squared distance between parameters and their expected values (regularisation with Gaussian prior).

2.3 Segmentation

MR images are segmented into different tissue classes using a modified Gaussian Mixture Model. By knowing the prior spatial probability of each voxel being grey matter, white matter or cerebro-spinal fluid, it is possible to obtain a more robust classification. Intensity non-uniformity correction is also used, which makes the method more applicable to images corrupted by smooth intensity variations.

The first step is to estimate the cluster parameters, then assign belonging probabilities and finally estimate the modulation function. The variance of each cluster (c) is computed:

$$c_k = \frac{\sum_{i=1}^{I} \sum_{j=1}^{J} p_{ijk} (f_{ij} u_{ij} - v_k)^2}{h_k} \text{ over k=1...K} \quad (3)$$

Bayes rule is used to assign the probability of each voxel belonging to each cluster:

$$p_{ijk} = \frac{r_{ijk} s_{ijk}}{\sum_{l=1}^{K} r_{ijl} s_{ijl}} \text{ over i=1…I, j=1…J and k=1…K} \quad (4)$$

To reduce the number of parameters describing an intensity modulation field, it is modelled by a linear combination of low frequency discrete cosine transform (DCT) basis functions. The modulation field U can be computed from the estimated coefficients (Q) and the basis functions (D1 and D2):

$$u_{ijk} = \sum_{n=1}^{N} \sum_{m=1}^{M} d_{2jn} q_{mn} d_{1im} \quad (5)$$

2.4 General Linear Model

A general linear model explains the response variable *y* in terms of a linear combination of the explanatory variables plus an error term:

$$y = x_1 \beta_1 + x_2 \beta_2 + e \quad (6)$$

The model implemented in the algorithm has a normally distributed and non-spherical error.

2.5 Statistical Inference

Hypotheses are tested using mainly one-way analysis of variance (ANOVA), one or two sample *t* tests and *F* tests depending on the type of analysis. Contrast vectors are established to make inquiries regarding the different regressors modelled on the design matrix in the general linear model. Test statistic t is computed:

$$T = \frac{c^T \hat{\beta}}{\sqrt{var(c^T \hat{\beta})}} = \frac{c^T \hat{\beta}}{\sqrt{\hat{\sigma}^2 c^T (X^T X)^{-1} c}} \sim t_{N-p} \quad (7)$$

The proposed algorithm uses ROI (Region of Interest) -based processing techniques to isolate the areas showing neural activity. The main characteristic of this method is that it utilises a binary mask to filter or perform operations on the desired pixels of an image. The binary mask is the same size as the image to be processed with pixels that define the ROI set to 1 and all other pixels set to 0. Several methods can be used for mask generation.

In this study we chose colour segmentation filtering, due to the characteristics of the input image, composed of two different types of information: a grayscale background showing the anatomical structure of the brain and skull of the subject and a red scale overlay containing the intensities and special extent of the neuronal activation. The implemented filter examines the values in the RGB matrix of the image

and extracts the pixels that fit in the range of colour values representing the cortical activity. The new image generated with these pixels form the mask that defines the ROI for our specific purpose. In order to identify and measure the different clusters of activated pixels we have used a contour detection technique for binary images. In our study case, this simple but effective method presents us with advantages over more complex ones, such as active contour models due to the characteristics of the input image. The possibility of using ROI segmentation to separate the areas of interest in a binary image allows the use of edge detection based on pixel connectivity, resulting in a faster and more precise classification of the detected clusters. Connected components are found and labelled by scanning the entire image searching for pixels with a value different from zero (which represents the background); all area and perimeter values for each cluster are also computed.

4. SYSTEM DESIGN

The system can be classified into two blocks, as shown in *Fig.1*. The first block uses SPM8 fMRI analysis routines to process and extract the information contained in the functional BOLD (Brain Oxygenation Level Dependent) images. The second block implements the cluster detection, feature measurement and results presentation.

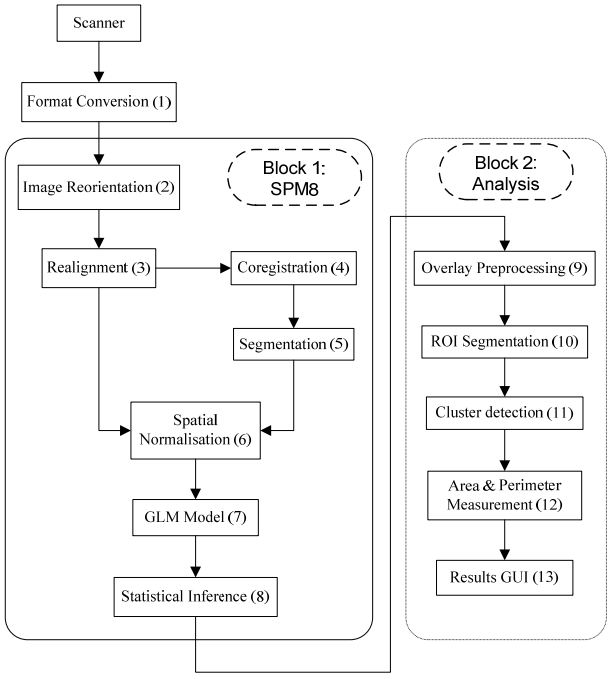

Figure 1 – fMRI analysis system block diagram.

The sequence of the process is as follows:

- Format conversion (1) from Siemens Magnetom format to Nifti-1 image format to be suitable for SPM8 processing. For this purpose we have chosen the MRIConvert tool due to its effectiveness and compatibility with Siemens proprietary format. Image header information is extracted and recoded according to the Nifti-1 standard.
- Reorientation (2) of the functional and structural images to equalize the origins of the coordinate systems. This step sets the images in the correct position with reference to the coordinate axis to match the position of the templates used in the spatial normalization steps. Odd results will appear after normalization if this correction is not included.
- Realignment (3) of the functional images to correct subject motion artefact during acquisition. Movements of the subject's head inside the scanner can alter the BOLD images inducing a change in the signal, which can be modelled using rigid body registration. The transformation uses a less square approach and consists of 3 rotations and 3 translations around and along the orthogonal axis [8].
- Co-registration (4) of structural and functional images. The within-subject registration method used here is based on work by Collignon et al [9] and it uses a rigid body model. The image that is assumed to remain stationary (sometimes known as the target or template image) is the mean of the realigned functional BOLD images, while the source image (structural T1 image) is moved to match it.
- Tissue segmentation (5) separates gray matter, white matter and cerebro-spinal fluid into different Nifti images for subsequent analysis. This step also implements bias-correction of the structural image and computes the deformation field parameters for spatial normalization [10]. The tissue probability maps used for segmentation were generated taking into account the age and gender of each study subject with the Template-o-Matic toolbox for SPM5 [11].
- Spatial normalization (6): the algorithm works by minimizing the sum of squares difference between the image which is to be normalized, and a linear combination of one or more template images. The primary use is for stereotactic normalization to facilitate inter-subject averaging and precise characterization of functional anatomy [12]. Smoothing using a Gaussian Kernel is also applied to the resulting normalized images in order to suppress possible noise signals.
- Model specification (7) according to the general linear model, which comprises the specification of the GLM design matrix, fMRI data files and filtering, and estimation of GLM parameters using traditional approaches.
- Statistical inference (8) and interrogation of results using contrast vectors to produce Statistical Parametric Maps (SPMs) and Posterior Probability Maps (PPMs). First (within-subject) and second (inter-subject) level analyses are tested using *F* tests and one or two sample *t* tests.
- Overlay pre-processing (9): the images showing structural anatomy with neural activation overlay are saved and arranged in mosaics to prepare them for feature extraction.
- ROI segmentation (10): neuronal activation results are extracted from the image applying a binary mask. The

mask is generated filtering the RGB matrix values with a predefined threshold.

- Cluster detection (11): the contour recognition algorithm labels and detects groups of activated voxels. The image is scanned to detect contiguous pixels and assign numeric labels to connected areas.
- Feature measurement (12): perimeter and area are computed for each cluster.
- GUI (13): measures can be accessed through an interface which allows the user to select the cluster to be analysed. Different subject or group results can be examined to find differences in areas of interest.

5. RESULTS

Intermediate and final results obtained for a healthy subject are shown in the figures below. The paradigm used was designed to activate the language areas of the subject, and it is composed of 90 complete volume scans, with a stimulus onset every 20 scans. Stimulus duration is of 10 scans. Parameters are corrected using FWE correction with a threshold value equal to $p<0.05$. *Fig. 2* shows a T1 (structural) and a functional BOLD image in the initial state (1), after reorientation, realignment and co-registration (2) and after the normalization and functional smoothing step (3). The fourth section in the figure shows the SPM (statistical parametrical map) computed and an overlay of the neuronal activation areas on the normalised T1 image.

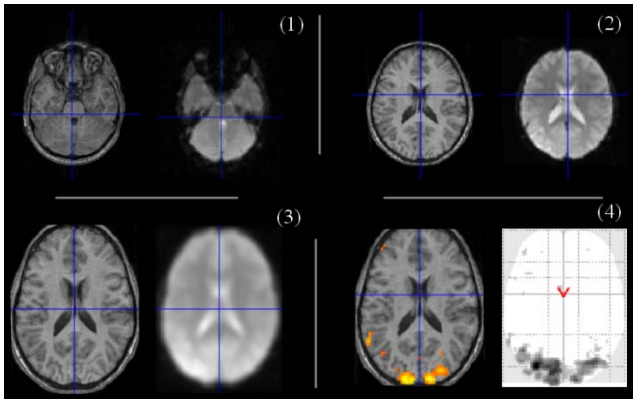

Figure 2 – fMRI analysis algorithm results.

Rigid body transformation parameters are shown in Fig. 3. Translation values are shown in mm along the x, y, and z axis during the acquisition of the different scanned volumes. At the same time, the subject's rotation movement around the axis is calculated and measured in degrees to model the artifact.

The analysis block begins with the generation of a 6x6 mosaic, choosing the specified slice separation on the horizontal plane which contains the areas relevant for the study of language-related neurological disorders, as shown in Fig.4.

Figure 3 – Realignment parameters.

Fig. 5 shows the binary mask resulting from the segmentation of the regions of interest using the RGB threshold technique.

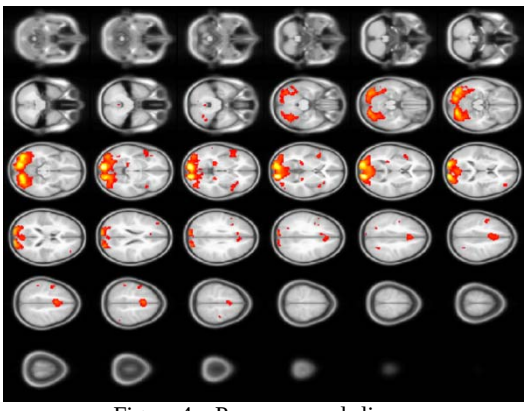

Figure 4 – Pre-processed slices.

The area and perimeter of each cluster is measured, and results are shown on an interactive user interface which allows the specialist to compare different studies for the same subject and extract conclusions on inferences between control and patient groups. An example of the latter is shown in *Fig.6.*

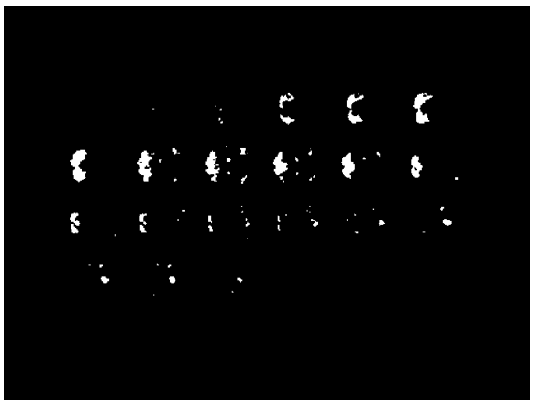

Figure 5 – ROI segmentation mask.

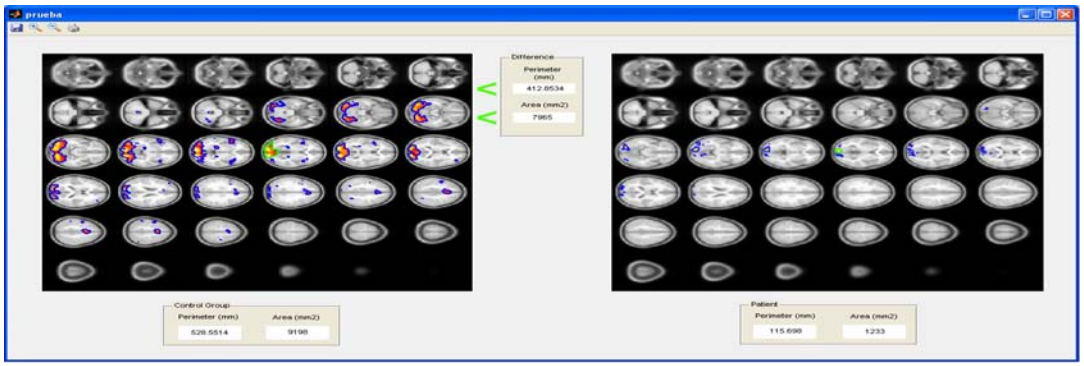

Figure 6 – Measures and comparison results.

Control group activations are shown on the left-hand side of the GUI, while the neural activity of a subject extracted from the patient group is situated on the right. The algorithm calculates the difference between areas and perimeters of the selected clusters belonging to the different maps and shows the results, as well as the respective parameter values of each object of the study.

6. DISCUSSIONS AND CONCLUSSIONS

Most of the success of the proposed system is due to SPM8 as a helpful tool for identifying activation regions. Being both control and patient group formed by young aged subjects the difficulty of obtaining clear and significant activations increases. Therefore the selection of an adequate processing tool is a key factor. Binary mask ROI segmentation results have been successful due to the input images characteristics. Grayscale structural background contrasts clearly with coloured activation areas, which makes this method preferable, as it is faster and more efficient than other tested techniques as Snakes or other active contour algorithms.

Quantitative parameters for the area and perimeter of the region under study have been automated by the algorithm, and manual measurement tests have been performed to check the validity of the results, with a relative error around 0.05%.

The possibility of comparison of two images from the same subject and different acquisition date will allow the specialists to make an objective evaluation of the treatment and assess the evolution of the patient.

Regarding objective fulfilling, regions of interest detection through fMRI processing has been successfully achieved, as well as the calculus of the objective numeric values related to the cortical activations.

In reference to the database objective, one of the future tasks to accomplish will be to add new samples that allow the validation of individual results and the expansion of the system to use it on a wider patient population profile. Finally, it would be interesting to integrate the system with EEG studies as a complementary tool to increase the amount of information about the neurological disorders under investigation.

7. ACKNOWLEDGMENTS

The authors wish to acknowledge Osatek for lending their infrastructures and materials. This work was partially financed by the Dep. of Industry and Dep. of Education, Universities and Research from the Basque Government

8. REFERENCES

[1] Birsh, Judith R. *"Research and reading disability"*. Baltimore, Maryland: Paul H. Brookes Publishing. pp. 8, 2005.

[2] Nair J, Ehimare U, Beitman BD, Nair SS, Lavin A. "Clinical review: evidence-based diagnosis and treatment of ADHD in children", *Mo Med*, vol.103, pp. 617–21, Nov-Dec 2006.

[3] Y. F. Taiand, P. Piccini, "Applications of positron emission tomography (PET) in neurology", *Journal of Neurology. Neurosurgery and Psychiatry*, vol.75, pp. 669-676, May 2004.

[4] Teresa Montez et al, "Altered temporal correlations in parietal alpha and prefrontal theta oscillations in early-stage Alzheimer disease", *Proc. of the National Academy of Sciences*, vol. 106, pp. 1614-1619, February 2009.

[5] Hynd et al, "Corpus Callosum Morphology in Attention Deficit-Hyperactivity Disorder: Morphometric Analysis of MRI", *Journal of Learning Disabilities*, vol. 24 pp.141-146, March 1991.

[6] A. M. Wink , J. Roerdink, "Extracting the Haemodynamic Response Function from fMRI Time Series using Fourier-Wavelet Regularised Deconvolution with Orthogonal Spline Wavelets", in *Proc. EUSIPCO 2006*, Florence, Italy, September 4-8. 2006

[7] The FIL methods group, "Statistical Parametrical Mapping", *http://www.fil.ion.ucl.ac.uk/spm/*.

[8] A. Collignon, F. Maes, D. Delaere, D. Vandermeulen, P. Suetens, and G. Marcha, "Automated multi-modality image registration based on information theory", in *Proc. Information Processing in Medical Imaging Conf. 1995*, Dordrecht, The Netherlands, October 21-28 1995, pp. 263-274.

[9] K.J. Friston, C. Frith, R.S.J. Frackowiak and R. Turner. "Characterizing dynamic brain responses with fMRI", *NeuroImage*, vol.2, pp .166-172, June 1995.

[10] J. Ashburner and K.J. Friston. "Unified segmentation", *NeuroImage*, vol. 26, pp. 839-851, July 2005.

[11] CCHMC (Cincinnati Children's Hospital Medical Center), "TOM toolbox", *https://irc.cchmc.org/software/tom.php*

[12] J. Ashburner and K.J. Friston, "The role of registration and spatial normalization in detecting activations in functional imaging", *Clinical MRI/Developments in MR*, vol.7, pp. 26-28, 1997.